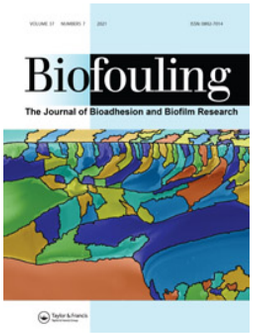

Taylor & Francis
Taylor & Francis Group

Biofouling
The Journal of Bioadhesion and Biofilm Research

ISSN: (Print) (Online) Journal homepage: https://www.tandfonline.com/loi/gbif20

Nanoscale characteristics of conditioning film development on photobioreactor materials: influence on the initial adhesion and biofilm formation by a cyanobacterium

Suvarna N. L. Talluri, Robb M. Winter & David R. Salem

To cite this article: Suvarna N. L. Talluri, Robb M. Winter & David R. Salem (2021) Nanoscale characteristics of conditioning film development on photobioreactor materials: influence on the initial adhesion and biofilm formation by a cyanobacterium, Biofouling, 37:7, 777-790, DOI: 10.1080/08927014.2021.1971201

To link to this article: https://doi.org/10.1080/08927014.2021.1971201

BIOFOULING
2021, VOL. 37, NO. 7, 777–790
https://doi.org/10.1080/08927014.2021.1971201

Taylor & Francis
Taylor & Francis Group

Nanoscale characteristics of conditioning film development on photobioreactor materials: influence on the initial adhesion and biofilm formation by a cyanobacterium

Suvarna N. L. Talluri[a,c], Robb M. Winter[a,b] and David R. Salem[a,b,c]

[a]Department of Chemical and Biological Engineering, South Dakota School of Mines and Technology, Rapid City, SD, USA; [b]Composites and Polymer Engineering Laboratory, South Dakota School of Mines and Technology, Rapid City, SD, USA; [c]Composite and Nanocomposite Advanced Manufacturing – Biomaterials Center (CNAM-Bio), South Dakota School of Mines and Technology, Rapid City, SD, USA

ABSTRACT

Adsorption of conditioning films on a solid surface is the first step in the development of biofilms. With the goal of understanding the preliminary adhesion mechanisms of cyanobacteria on photobioreactor (PBR) materials to prevent biofouling, the physical changes occurring on PBR materials were investigated during the initial adhesion and biofilm formation by *Anabaena* sp. PCC 7120, a cyanobacterium that is genetically modified to produce linalool. Atomic force microscopy (AFM) revealed that the conditioning film deposition was in the form of spike-like structures on all the materials except PVC. The average heights (in the range 9 – 16 nm) of the conditioning films deposited on glass, PMMA, PC and HDPE were 11 to 20 times higher than on PVC at 96 h. The time dependent change in thickness of conditioning films correlated well with *Anabaena* cell attachment to the PBR materials. The rapid and significant colonization of *Anabaena* on glass within 48 h was consistent with the increase in thickness of the conditioning film within this time period. Lack of the conditioning film spike structures and no change in thickness of the conditioning films with time on the PVC together with comparatively delayed cell attachment and conditioning-film protein deposition on this material, indicated that the nanoscale spike structures on the other PBR materials may be accelerating the cell attachment process but are not a prerequisite for cell attachment. These results suggest that PVC should be explored further as an antifouling material for photobioreactors. The thickness of the conditioning films on glass measured by a scratch and scan method was in good agreement with the thickness values measured by an adhesive tape method, indicating that both these methods can be used for fast and reliable AFM thickness determination of bacterial conditioning films.

ARTICLE HISTORY
Received 21 March 2021
Accepted 15 August 2021

KEYWORDS
Biofouling; biofilms photobioreactors; conditioning films; atomic force microscope; cyanobacteria; adhesion mechanisms

Introduction

Biofouling is a pervasive and problematic phenomenon occurring on materials where bacteria are prevalent, especially in aquatic environments (Bixler and Bhushan 2012), and it can often cause failure of equipment and devices (Preedy et al. 2014). Examples include biofilm colonization on medical devices, microbial corrosion on industrial equipment, biofilms in food processing equipment (Preedy et al. 2014) and biofouling on ship hulls (Thome et al. 2012). In addition, microalgal biofouling in photobioreactors reduces the light transmission efficiency of the photobioreactor (PBR) wall materials leading to decreased algal biomass productivity (Brennan and Owende 2010; Dasgupta et al. 2010; Dragone et al. 2010; Harris et al. 2013; Talluri et al. 2020), and requiring frequent shut down of the PBRs for cleaning (Harris et al. 2013; De Vree et al. 2015; Talluri et al. 2020). Cyanobacterial based biofuel production is gaining importance due to its ability to utilize CO_2 and sunlight to produce O_2 and high value chemicals (Parmar et al. 2011; Talluri et al. 2020), but only a few reports are available on antifouling technologies for the PBRs (Wang et al. 2017; Zeriouh et al. 2017, 2019; Talluri et al. 2020), and studies on bioadhesion and the biofouling mechanisms of cyanobacteria on PBR materials are lacking.

In the complex, multi-step process of biofouling, adsorption of dissolved organic matter onto the materials is considered the first step, known as conditioning film formation (Francius et al. 2017). The deposited conditioning films modify the surface

CONTACT David R. Salem David.Salem@sdsmt.edu; Robb M. Winter Robb.Winter@sdsmt.edu

physico-chemical properties of the materials, such as roughness, surface charge, chemistry, and surface energy within a few minutes to hours, which influences subsequent bacterial adhesion and biofilm formation (Thome et al. 2012; Francius et al. 2017; Talluri et al. 2020). Most of the current literature on conditioning films has focused on determining their elemental chemical composition by X-ray photoelectron spectroscopy (XPS) (Compere et al. 2001; Hwang et al. 2012a, Hwang et al. 2012b, 2013; Yang et al. 2016) and their surface chemical functional groups by Fourier transform infrared (FTIR) spectroscopy or Infrared Reflection Absorption Spectroscopy (IRRAS) (Ladner et al. 2010; Lorite et al. 2011; Thome et al. 2012; Talluri et al. 2020). Studies have shown that in addition to the surface chemistry, the physical nature of the conditioning films deposited on materials could also play an important role in the early adhesion process (Compere et al. 2001; van der Aa and Dufrene 2002; Francius et al. 2017).

Given that conditioning films are in the order of a few nanometers in thickness (Thome et al. 2012), atomic force microscopy (AFM) provides a useful technique to explore their physical nature in three dimensions. Although both AFM and spectral ellipsometry (Thome et al. 2012, 2014) are non-destructive techniques that can be used to measure conditioning film thickness, the thickness calculations used in spectral ellipsometry are not straightforward (Hong et al. 2011). AFM, on the other hand, offers many comparative advantages such as high vertical resolution (< 0.1 nm), and no prior knowledge is needed of the physical properties of the conditioning films (Lobo et al. 1999; Hong et al. 2011; Pascu and Dinescu 2012; Francius et al. 2017). AFM also permits quantitative characterization of interfaces, a morphological view of the surface (Gesang et al. 1995), and relatively fast image acquisition time (Beech et al. 2002). Moreover, three-dimensional topographical information obtained at higher resolution (Gazze et al. 2013) can help to provide a mechanistic understanding of conditioning film formation at the nanoscale.

In this study, AFM was used to investigate the physical nature of the conditioning films deposited on PBR materials and its influence on initial adhesion of *Anabaena* sp. PCC 7120, a filamentous nitrogen fixing cyanobacterium with the ability to survive high levels of CO_2 (Thomas et al. 2005), and an excellent host for the production of high value chemicals and the removal of heavy metals from industrial wastewater (Ruffing 2011). The *Anabaena* sp. PCC 7120 used in the present study was genetically engineered to produce oxygen and linalool (a platform chemical) directly from CO_2 and sunlight, for potential application in space colonizing missions (Duke 2011; Zhou and Gibbons 2015). As described by Wang et al. (2012), the design criteria for PBRs, whether of the flat panel or the tubular type, require wall materials that satisfy the transparency requirements as well as the mechanical properties for PBR construction. Widely used PBR materials that satisfy these basic requirements are glass, polyvinyl chloride (PVC), poly (methyl methacrylate) (PMMA), polycarbonate (PC) and, most commonly, polyethylene (PE) (Wang et al. 2012; Genin et al. 2014). These materials were therefore used as model substrata in the present study and in a related report (Talluri et al. 2020). Here, the focus is on characterization of the surface roughness, thickness and topography changes resulting from the deposition of the conditioning films on these PBR materials, before and during the initial attachment of the engineered *Anabaena* (for up to 96 h), with the goal of gaining insights into the influence of conditioning films on microbial adhesion mechanisms. This knowledge may ultimately help to devise strategies to prevent *Anabaena* adhesion and the resulting biofilm formation.

Materials and methods

Materials and preparation

For the glass substratum, soda lime glass microscope slides ($25 \times 75 \times 1$ mm) (Cat. No. 12-544-4) were purchased from Fisher Scientific (Pittsburgh, PA, USA). The polymer substrata materials, purchased from Goodfellow Corporation (Coraopolis, PA, USA), were poly (methyl methacrylate) (PMMA) (Cat. No. 531-676-08), poly vinyl chloride (PVC) unplasticized (Cat. No. 560-572-61), polycarbonate (PC) (Cat. No. 646-279-93), and high-density polyethylene (HDPE) (Cat. No. 894-690-40) sheets (thickness of 1 mm). Further information on the properties of these transparent polymer materials can be found at http://www.goodfellowusa.com. All the materials were cut into coupons of 50×15 mm. Glass coupons were sonicated in 1 N HCl for 10 min, vigorously rinsed in deionized water, 70% alcohol and again rinsed with deionized water (Hwang et al. 2012b). All the polymer coupons were rinsed in 70% ethanol followed by vigorous rinsing in deionized water (Cui et al. 2013). After the cleaning procedure, all the substratum coupons were stored in a flask containing sterile deionized water until used for experiments.

Cyanobacterium and culture conditions

A genetically engineered cyanobacterium, *Anabaena* sp. PCC 7120 which produces a high value chemical, linalool, was used as a model cyanobacterium in this study (Zhou and Gibbons 2015). Linalool producing *Anabaena* (engineered *Anabaena*) was provided by Drs R. Zhou and W. Gibbons of the Biology and Microbiology department at South Dakota State University, Brookings, SD. The strain was cultured in modified BG-11 medium containing 1.5 g of $NaNO_3$, 0.0366 g of $MgSO_4 \bullet H_2O$, 0.036 g of $CaCl_2 \bullet 2H_2O$, 0.04 g of $K_2HPO_4 \bullet 3H_2O$, 0.006 g of citric acid, 0.006 g of ferric ammonium citrate, 0.001 g of EDTA (disodium magnesium salt), 0.02 g of Na_2CO_3 and 1 ml of trace element mix A5 + Co dissolved in 1 l of deionized water. The trace element mix A5 + Co solution contained 2.86 g of H_3BO_3, 1.81 g of $MnCl_2 \bullet H_2O$, 0.222 g of $ZnSO_4 \bullet 7H_2O$, 0.39 g of $Na_2MoO_4 \bullet 2H_2O$, 0.079 g of $CuSO_4 \bullet 5H_2O$, 0.0494 g of Co $(NO_3)_2 \bullet 6H_2O$ dissolved in 1 l of deionized water (Rippka et al. 1979; Zhou and Gibbons 2015). The initial pH of the modified BG-11 medium was 7.1. The engineered *Anabaena* was inoculated in 200 ml sterile BG-11 medium containing 100 µg ml^{-1} neomycin and incubated at 30 °C at 150 rpm in an orbital incubator shaker under the light intensity of 25-30 microeinsteins m^{-2} s^{-1} (Rippka et al. 1979; Zhou and Gibbons 2015). Throughout the study, the engineered *Anabaena* was cultivated under atmospheric air until the culture reached the exponential phase (optical density between 0.7 − 0.8).

Initial adhesion of genetically engineered cyanobacterium to PBR materials

A method described by Irving and Allen (2011) and modified by Talluri et al. (2020) was used to conduct the initial adhesion and biofilm formation assay of genetically engineered *Anabaena*. Agar media were prepared by adding 1% agar in BG-11 medium and sterilized by autoclaving at 121 °C for 20 min. Neomycin (100 µg ml^{-1}) was added to the sterile agar media and 30 ml of the agar medium was poured into several 100 mm large Petri dishes. The agar was cut with a sterile scalpel blade and glass and the polymer coupons of 50 × 15 mm were securely inserted. Three replicate Petri dishes were prepared for each time interval and material in a similar manner and 30 ml of engineered *Anabaena* cell suspension (8×10^7 cells ml^{-1}) containing 100 µg ml^{-1} neomycin were added to the Petri dishes. The dishes were incubated at 30 °C under the light intensity of 25-30 microeinsteins m^{-2} s^{-1} without shaking. Three replicate coupons were retrieved for all the materials at each time interval up to 4 days during the course of engineered *Anabaena* adhesion tests (Irving and Allen 2011; Talluri et al. 2020). The coupons were gently rinsed in deionized water to remove loosely bound cells, air dried at room temperature overnight (Irving and Allen 2011; Talluri et al. 2020) and analyzed by atomic force microscope as described in the following section. The images of engineered *Anabaena* cells adhered to the PBR materials were captured by using an upright microscope (Carl Zeiss Axio Imager.M1m, Thornwood, NY, USA), processed in ImageJ (Rasband 1997) and the percentage area coverage of *Anabaena* on the different PBR materials was calculated (Talluri et al. 2020). Additional details about the ImageJ processing and calculation of mean percent area coverage of engineered *Anabaena* can be found in Talluri et al. (2020).

Atomic force microscopy (AFM)

Surface topography and phase images of the PBR materials subjected to an adhesion assay for up to 96 h were captured by a multimode atomic force microscope (Multimode 8, Bruker, Santa Barbara, CA, USA). The AFM was operated in tapping mode using a silicon probe purchased from Bruker AFM probes (Bruker AFM probes, Camarillo, CA, USA) with a spring constant of 3 N m^{-1}, a height of 15-20 µm, a radius of 8 nm, and a resonance frequency of 75 KHz. The surface topography and phase images of all the materials were obtained with a maximum scan area of 13.5 µm × 13.5 µm or 10 µm × 10 µm with E scanner. At least five random locations from each of the three replicate coupons were captured by AFM to determine the surface roughness of the PBR materials during *Anabaena* adhesion at different times. Images were processed in Nanoscope 8.15 software using Flatten and Clean Image commands prior to the analysis (Auerbach et al. 2000). Clean Image command was applied to smooth the noisy image and Flatten command was applied to eliminate the noise, bow and tilt of the images. Roughness analysis function was applied to calculate the root-mean-squared (R_q) roughness of the conditioning films deposited on PBR materials (Auerbach et al. 2000; Lorite et al. 2011).

A scratch and scan method (Uzum et al. 2012) was used to determine the height and thickness of the conditioning films deposited during adhesion of the engineered *Anabaena*. A long narrow scratch a few tens of nanometers in depth was made in the middle

of the PBR material coupons using a size 5 sewing needle (Dritz needle compacts, SC, USA) (Uzum et al. 2012) with the intent of penetrating the conditioning film down to the surface of the substratum. At least three images from each of the three replicates were captured along the length of the scratch on all the materials at different times. Analysis functions such as section and step were performed on the topography images to determine the height and thickness of the conditioning films deposited on the different PBR materials (Auerbach et al. 2000; Lorite et al. 2011). In section analysis, the *height* of the conditioning films (R_z) was calculated as the average difference in *height* between the five highest peaks and the five lowest valleys relative to the center line. In step analysis, the scratch was assumed to create a step between the top of the conditioning film and the exposed PBR surface (without conditioning film). The average vertical distance between the two regions was calculated as the *thickness* of the conditioning film deposited on the materials.

A sticky tape method (adhesive tape method) was conducted on glass to test the validity of the scratch and scan method (Anderson 2009). To conduct this method, an engineered *Anabaena* adhesion assay was carried out as described in the previous section. Briefly, the glass substratum was cut into three replicate coupons of 25 × 15 mm and masked at the edge with a clean adhesive tape under aseptic conditions and incubated in the engineered *Anabaena* suspension for 96 h. The coupons were retrieved from the growth medium at 96 h, washed gently in deionized water to remove loosely bound cells and air dried overnight. The adhesive tape was carefully removed from the glass coupons and the area that covers both the conditioning film and the edge of the footprint of the adhesive tape was scanned in three different locations along the edge on each replicate coupon. Step analysis was conducted on the resulting topography images and the thickness of the conditioning films was determined.

Statistical analysis

Mixed analysis of variance (mixed ANOVA) was conducted to evaluate the statistically significant differences in mean surface roughness and thickness of conditioning films deposited on the PBR materials at different time intervals. At 96 h, the statistical differences in average height (R_z) of the conditioning films on different PBR materials and the thickness of the conditioning films on glass measured by the scratch and scan method and adhesive tape method were evaluated by univariate analysis of variance (Univariate ANOVA). ANOVA was conducted followed by Tukey's *post hoc* test for multiple comparisons of means with Bonferroni correction. Replicate coupons were nested within each material for all the time intervals. Statistical analyses were conducted using SPSS v27.0 statistical software.

Results and discussion

Conditioning films are biomolecules that are exuded by microbial cells in suspension and can also be exuded by the cells during their exploration of the surface for initial attachment. In the authors' previous study on conditioning films and initial adhesion of *Anabaena* on the PBR materials, based on FTIR spectroscopy, optical microscopy visualization, and contact angle measurements, no indication was found of cell attachment until after 12 h on any of the materials tested (Talluri et al. 2020). Therefore, conditioning films detected in the 6 h − 12 h interval are entirely attributed to exudate from suspended or surface exploring microbes. Evidence of reversible cell attachment started to be detected at 24 h on some of the materials, in the form of patches of residual extracellular polymeric substances (EPS); and the glass substratum even showed a small amount of irreversible cell attachment at this time interval (Talluri et al. 2020). Initial, irreversible colonization by the *Anabaena* on the polymer PBR materials occurred in the range of about 72 h; and by 96 h, all the substrata showed varying degrees of irreversible cell adhesion and early-stage biofilm development. The evolution of cell adhesion for the different substrata is summarized quantitatively in Figure 2 (adapted from Talluri et al. 2020), in terms of area covered by the cells.

In the present study, AFM was used to investigate the physical nature of the conditioning films deposited on photobioreactor materials, before and during the initial adhesion of engineered *Anabaena* for up to 96 h. Surface topography and phase images were acquired from the PBR materials retrieved from *Anabaena* suspension at different time intervals (12, 24, 48, 72 and 96 h) within the conditioning and cell attachment regimes described above. Physical properties such as surface roughness, height and thickness of the conditioning films were measured. While processing the images in the software, only cell-free areas were taken into consideration (Beech et al. 2005) in order to specifically observe the nanoscale changes occurring on materials due to adsorption of

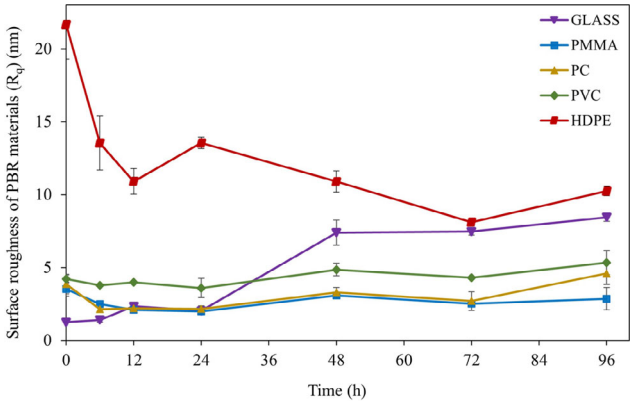

Figure 1. Change in root-mean-squared (R_q) roughness of the cell free areas of different PBR materials with time during the initial adhesion of engineered *Anabaena*. Values at the zero time scale represents the roughness (R_q) of clean PBR materials. Error bars represent the standard errors (SEs) of the mean (n = 3). The mean roughness and SE were calculated based on three independent means at each time interval for all the PBR materials.

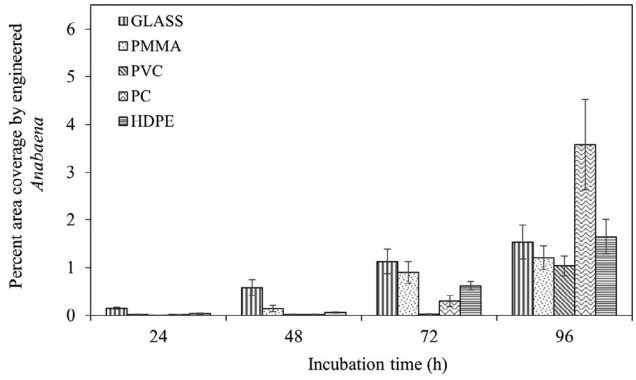

Figure 2. Initial adhesion of engineered *Anabaena* cells on different PBR materials with time. Error bars represent ± SEs (n = 3). The mean percentage area coverage and the SE were calculated based on three independent means at each time interval for all the materials. Reproduced with permission from Talluri et al. 2020 (Biofouling 36: 183–199) and Taylor & Francis.

conditioning films during adhesion of the engineered *Anabaena*. Clearly, conditioning film measurements taken on samples after immersion for 12 h in the suspension may include exudate biomolecules from both the suspended cells and the adhered cells, and no attempt was made to distinguish these contributions.

Figure 1 shows the time course change in root-mean-squared roughness (R_q) of the PBR materials during the adsorption of conditioning films. Mixed ANOVA results revealed that there were statistically significant differences in the average roughness between different PBR materials $F(4,60) = 733.49$, $p < .001$ and across different time intervals $F(4.295,257.71) = 30.07$, $p < .001$. There was a significant interaction effect between the time and material $F(17.18,257.71) = 41.87$, $p < .001$. A significant decrease in roughness of HDPE within 6-12 h (Tukey's test, $p < .05$) was observed. The roughness of glass, PMMA, PVC and PC did not significantly change between 0-12 h (Tukey's test, $p > .05$). Between 12 h and 96 h, 3.6-fold and 2.1-fold increases in the surface roughness of glass and PC (Tukey's test, $p < .05$) were observed. On the other hand, the roughness of PMMA and PVC between 12 h and 96 h was unaffected during the *Anabaena* adhesion process. These results indicate that the adsorption of conditioning film appears to smooth the surface of the material with the roughest surface (HDPE) within the first 12 h (decreasing R_q from about 22 nm to about 11 nm), while not significantly affecting the surface roughness of the other substrata, which had much lower initial R_q values, in the approximate range $1 - 4$ nm.

From Figure 2, it is clear that *Anabaena* cells were able to adhere to all the surfaces (see also, Talluri et al. 2020). While it is not clear whether the reduction in surface roughness was a prerequisite for *Anabaena* cell attachment in the case of the HDPE substratum, it is evident that *Anabaena* cells were able to adhere to the other PBR surface materials without surface roughness being significantly altered by adsorption of the conditioning films.

The representative topography and phase images of glass obtained from the scratch and scan method and the respective line profiles obtained from section analysis of the topography images at different times are displayed in Figure 3, and illustrate the time dependent evolution of conditioning films on glass during the initial adhesion of *Anabaena* up to 96 h. The presence of conditioning film was evident on glass in the form of spikes with heights (R_z) increasing with time (Figure 3), and it is evident that the conditioning film adsorption continued during the adhesion of *Anabaena* to glass. It was found that even though the conditioning film spikes were present on glass within 6 h (data not shown) there was no significant difference in heights ($R_z \sim 2$ nm) of the conditioning film spikes between 6 h and 12 h on glass.

Along with the conditioning film spikes, an indication of encapsulating (or capsule-like) structures (shown with arrows) was observed around the *Anabaena* cells in the topography and phase images of the glass-substratum samples (Figure 4). Two primary classifications of extracellular polysaccharides are capsular polysaccharides (CPS), where the polysaccharide is intimately bound to the cell wall, and slime polysaccharides, where the polysaccharide is

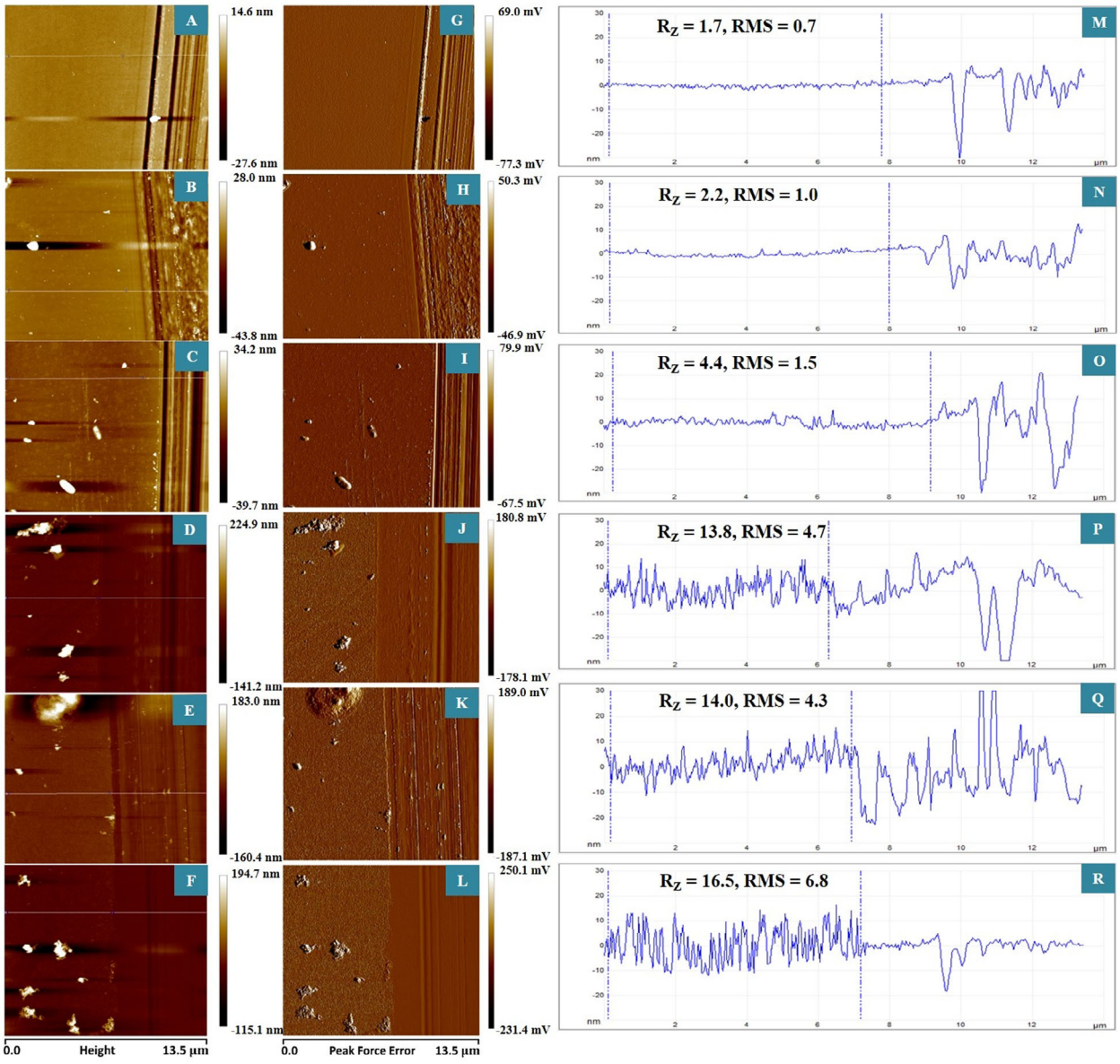

Figure 3. Representative AFM topography (A, B, C, D, E and F) and phase (G, H, I, J, K and L) images of glass incubated in an engineered *Anabaena* suspension for 0 h (A and G), 12 h (B and H), 24 h (C and I), 48 h (D and J), 72 h (E and K) and 96 h (F and L). The left side of the topography and the phase images indicated with blue markers on the line represent the area of clean glass surface/conditioning film deposited on glass surface at different times. The right side of the image represents the scratch made on glass using a sewing needle. Line profiles (M, N, O, P, Q and R) resulting from section analysis of topography images show the evolution of conditioning film on glass with time and the respective R_z and RMS values. R_z is the ten-point mean roughness between the reference markers which is defined as the average difference in height between the five highest peaks and the five lowest valleys relative to the center line. RMS is the SD of the Z values between the reference markers. All the images were obtained with a scan area of 13.5 µm × 13.5 µm. R_z and RMS values are reported in nanometers.

dispersed or loosely associated with the cell (De Philippis and Vincenzini 1998; De Philippis et al. 2001). The CPS observed on the glass substratum may be assisting in the adhesion of *Anabaena* to glass. A similar observation was reported by Lorite et al. (2013) during the early stages of *Xylella fastidiosa* biofilm formation on glass. Interestingly, in the present study, there was no evidence of capsule structures around the cells deposited on the polymer substrata during *Anabaena* adhesion. While a definitive explanation for this difference in behavior cannot be provided at this stage, it could be associated with the very hydrophilic nature (CA ∼ 17°) of glass, compared with the polymer PBR materials which had contact angles between 85°and 93° (Talluri et al. 2020). There are two stages in the adhesion of bacteria to a surface: reversible adsorption, occurring at the secondary minimum in surface interaction energy

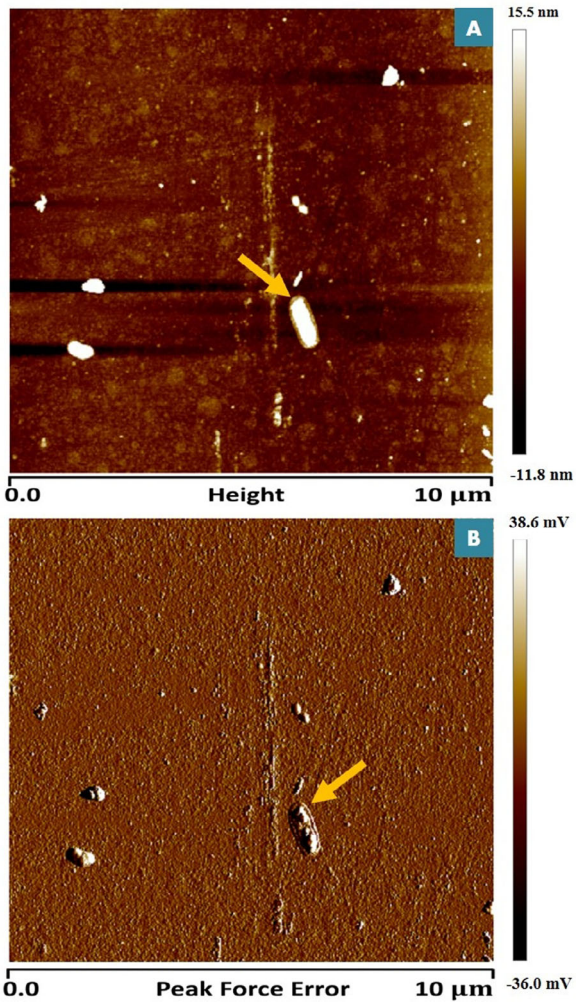

Figure 4. AFM topography (A) and phase (B) images of glass incubated in engineered *Anabaena* suspension for 24 h. Images were obtained with a scan area of 10 µm × 10 µm.

(~15 nm from the surface), and irreversible adsorption occurring at the primary minimum, ~ 1 nm from the surface (Oliveira 1992). In some cases, the cell may use EPS, including the capsular form, to assist in bridging the distance between the secondary and primary minima (Oliveira 1992). For the glass surface, unlike the polymer surfaces, there is a lack of hydrophobic interactions capable of overcoming repulsion from the overlap of negative charges on the cell surface and conditioning film. Therefore, in the absence of significant assistance from hydrophobic interactions, the *Anabaena* cells may produce CPS as a strategy to transverse the secondary and primary minima near the hydrophilic surface of the glass. Furthermore, the results of the related FTIR study (Talluri et al. 2020) revealed that, between 12 h and 48 h, the polysaccharide deposition was about 2 to 8 times higher on glass than on the polymer substrata, supporting the notion that the cells favored utilization of EPS for adhesion to the glass substratum and less so, or not at all, for adhesion to the polymer substrata. Indeed, the adhesion assay revealed that rapid adhesion of *Anabaena* cells occurred on glass within 24 h, compared with no irreversible attachment on the other materials until at least 48 h (Talluri et al. 2020). However, it should also be pointed out that a bacterium can produce more than one type of adhering polymer in response to different surface chemistries and different stages of biofilm development (Costerton et al. 1978; Mody et al. 1990; Ong et al. 1990). It is therefore possible, for example, that the cyanobacterium might have produced chemically different CPS when initiating cell adhesion to glass and polymers, such that rinsing the substratum coupons in distilled water dissolved any CPS surrounding the cells on polymer substrata but was unable to dissolve the CPS surrounding the cells on the glass surface. In any case, further investigation of the chemical nature of different capsular polysaccharides released in response to adhesion of cyanobacteria to substrata with different surface chemistries may lead to a better understanding of the absence or presence of CPS around the *Anabaena* cells on these surfaces.

The heights of the conditioning films deposited on glass and the different polymer materials at 96 h were compared, and representative images are displayed in Figure 5. At 96 h, the average height of the conditioning films deposited on glass (~ 15.8 nm), PC (~ 14.1 nm), HDPE (~ 15.5 nm) and PMMA (~ 8.9 nm) was substantially higher than on PVC (~ 0.8 nm) (Tukey's test, $p < .05$ for each combination). Figure 2 shows the higher *Anabaena* cell attachment on PC (~3.6%) and HDPE (~1.6%) than on PVC (~1.0%), but no significant difference in the percentage area coverage of *Anabaena* was found between glass (~1.5%), PMMA (~1.2%) and PVC (~1.0%) (Talluri et al. 2020). These results indicate that there was no direct correlation between the heights of the conditioning films deposited on the PBR materials after 96 h and the level of *Anabaena* cell attachment within this time period. However, a qualitative observation of several AFM topography and phase images of PVC revealed little to no indication of the conditioning film spikes on PVC, unlike the other PBR materials (Figure 5).

In the related FTIR study (Talluri et al. 2020), the presence of proteins and polysaccharides before and during the initial attachment of *Anabaena* on these PBR materials was reported. Therefore, the spikes/dot-like structures observed on PBR materials in this study (Figure 5) are likely to be conditioning films

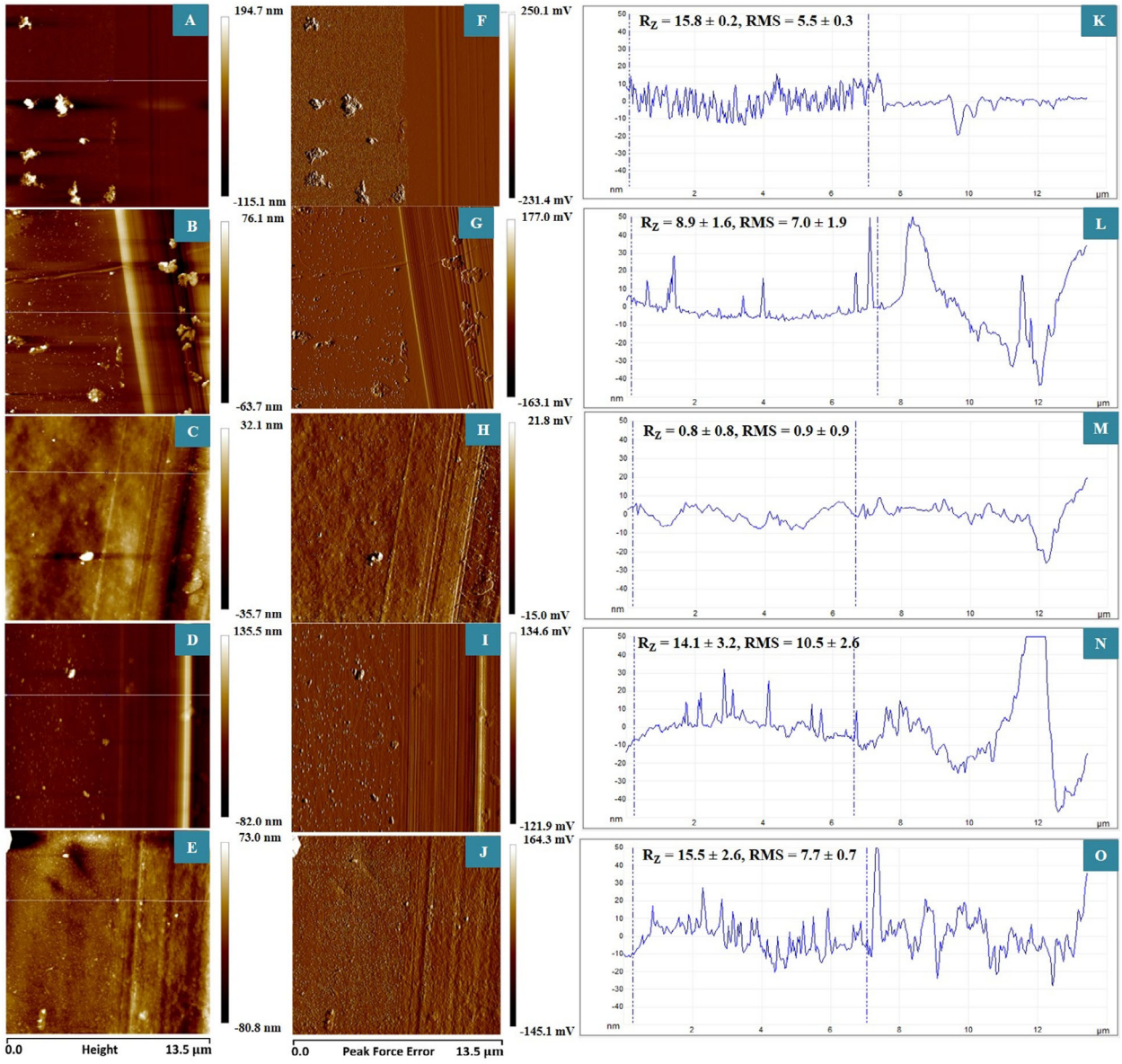

Figure 5. Representative AFM topography (A, B, C, D and E) and phase (F, G, H, I and J) images of glass (A and F), PMMA (B and G), PVC (C and H), PC (D and I) and HDPE (E and J) incubated in engineered *Anabaena* suspension for 96 h. The left side of the topography and phase images indicated with blue markers on the line represent the area of conditioning film deposited on glass/polymers at 96 h. The right side of the image represents the scratch made on glass/polymers using a sewing needle. The line profiles (K, L, M, N and O) obtained from section analysis of topography images show the conditioning films developed on glass (K), PMMA (L), PVC (M), PC (N) and HDPE (O) at 96 h. R_z and RMS values displayed were obtained from section analysis conducted on at least 3 images (5 different locations within each image) from each of the three replicate coupons for all the materials. R_z and RMS values were reported as mean ± SE of the three-independent means (n = 3) in nanometers. All the images were obtained with a scan area of 13.5 µm × 13.5 µm.

consisting of proteins and polysaccharide molecules. Interestingly, the FTIR study showed that conditioning film proteins were present on glass, PMMA, HDPE and PC within 12 h, whereas they were not evident on PVC until 48 h, and increased only modestly on this surface after about 84 h. The relatively constrained development of conditioning film proteins on PVC may be associated with the lack of the spikes/dot-like structures on the PVC substratum, which may in turn be responsible for the delay in the onset of colonization of the engineered *Anabaena* on this surface until about 72 h (Figure 2).

On glass, the conditioning films appeared as uniformly distributed spikes having close association with one another, whereas in the case of PMMA, PC and HDPE, they appeared as isolated dot-like structures of varying heights (Figure 5). Somewhat similarly, an AFM study of the surface of a stainless-steel

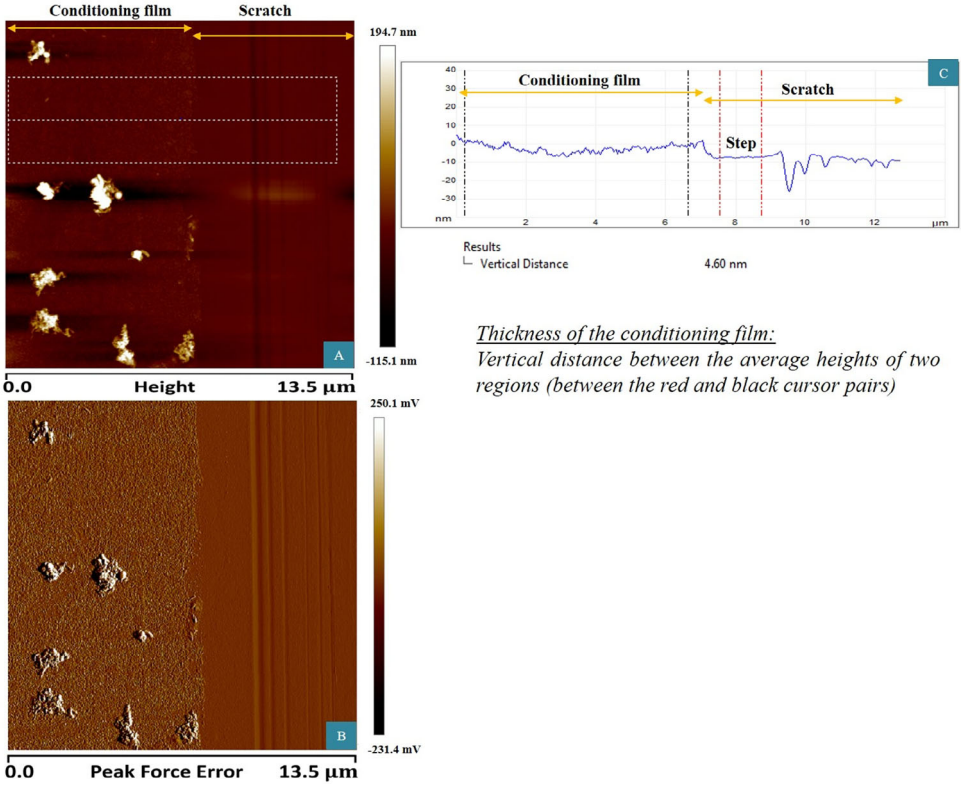

Figure 6. Representative AFM topography (A) and phase (B) images of glass obtained from the scratch and scan method. The left side of the image represents the conditioning film deposited on glass. The right side of the image shows the scratch created using a needle. The box indicated with the dashed lines in the topography image represents the region used for step analysis. (C) shows the result of the step analysis within this region (box with dashed lines). The region between the red markers where damage to the glass by the needle appeared minimal was used as a step to determine the thickness of the conditioning film spikes. The vertical distance between the average heights of the two regions (between the red and black markers) is referred to as the thickness of the conditioning film deposited on the materials. Images were obtained with a scan area of 13.5 µm × 13.5 µm.

substratum that had been immersed in seawater (Compere et al. 2001) revealed a heterogeneous coverage of conditioning films in the form of particles of various sizes, which became denser with time. van der Aa and Dufrene (2002) studied the surface of a polystyrene substratum after the adhesion of the *Azospirillum brasilense* bacterium and observed the presence of dot-like structures protruding from a continuous layer of adsorbed proteins, attributed to the adsorbed proteinaceous EPS. Whereas the particulate or spike-like conditioning film morphologies that have been observed are expected to influence cell attachment by, for example, creating high surface area adhesion sites, their level of importance in ensuring effective cell attachment is not well understood. The observations in the present study of an essentially featureless conditioning film surface on PVC together with the delayed onset of cell attachment on this substratum compared with the other PBR materials, imply that the spikes or dot-like conditioning film morphologies may aid or accelerate cell attachment but are not a prerequisite.

Step analysis was performed on AFM topography images obtained from the scratch and scan method to determine whether the thickness of the conditioning layer deposited on PBR materials has an influence on *Anabaena* attachment. Step analysis of a representative AFM topography image is shown in Figure 6. Table 1 shows the change in thickness of the conditioning film with time on different PBR materials determined by the scratch and scan method. The thickness of the conditioning films after 96 h was found to be ∼ 8.0 nm on glass, 7.2 nm on HDPE, 6.2 nm on PC, 3.4 nm on PMMA and 3.8 nm on PVC. Being < 10 nm in all cases, these numbers are consistent with the thickness values of the conditioning films reported in the literature (Lorite et al. 2011; Thome et al. 2012).

Between 12 and 48 h, the thickness of the conditioning films increased by 2.2 times on glass, whereas for the other materials, the change in conditioning film thickness was not significant during this time period (Table 1). This could be the reason for rapid colonization and higher percentage area coverage of

Table 1. Thickness of the conditioning film deposited on PBR materials obtained by the scratch and scan method.

Time (h)	Thickness of the deposited film (nm)				
	Glass	PMMA	PVC	PC	HDPE
12	2.9 ± 0.6	1.2 ± 0.1	2.8 ± 0.3	3.4 ± 0.7	5.3 ± 0.6
48	6.4 ± 0.5	2.1 ± 0.5	3.1 ± 0.8	4.3 ± 0.8	5.4 ± 0.5
96	8.0 ± 0.2	3.4 ± 0.6	3.8 ± 0.5	6.2 ± 0.5	7.2 ± 0.7

Values represent the means ± the SEs of the three-independent means (n = 3). Mixed ANOVA results revealed significant changes in the thickness of the conditioning films between different PBR materials $F(4,30) = 15.06$, $p < .001$ and across different time points $F(2,60) = 22.48$, $p < .001$.

the engineered *Anabaena* cells on glass (~ 0.6%) than on any other PBR materials (~ 0.1% or less) at 48 h (Figure 2) (Tukey's test, $p < .05$ for each combination). It also supports the finding that the conditioning film spikes were observed on glass within 6 to 12 h whereas on the other materials (except for PVC) the spikes/dot-like structures were observed at around 48 h (data not shown). A significant increase in thickness of the conditioning films on PMMA (2.8 times), PC (1.8 times) and HDPE (1.4 times) occurred between 12 and 96 h (Table 1) (Tukey's test, $p < .05$), and qualitative interpretation of AFM images suggests that the conditioning film structures deposited were denser at 96 h than at 48 h on these materials. This could be the reason why colonization of *Anabaena* did not occur as rapidly and significantly on PMMA, PC and HDPE as on glass, until after 48 h (Figure 2). These results indicate that initial adhesion of *Anabaena* occurs after the accumulation of these conditioning film structures, which may be altering the physical properties of the surface to provide anchoring points or adhesion sites for the cyanobacterium, to facilitate the adhesion process. The density of these conditioning film structures and the time of deposition may be crucial for facilitating the adhesion process of *Anabaena*. Interestingly, no significant increase in the thickness of the conditioning films on PVC between 12 and 96 h (Table 1) (Tukey's test, $p > .05$) was observed, which appears consistent with the infrequent occurrence of detectable conditioning film structures, in the form of spikes or dots, in the AFM images and AFM line profile of Figure 5. These results indicate that the time dependent change in the thickness of the nanoscale conditioning films correlated reasonably well with the attachment behavior of *Anabaena* on PBR materials. Together, these results suggest that the thickness of the conditioning films as well as their spatial and topological organization are important determinants of the rate and extent of the initial adhesion of *Anabaena*. In this regard, the study provides evidence that, while the spike-like conditioning film morphology does not seem to be a prerequisite for *Anabaena* cell attachment, these nanoscale structures may accelerate the rate of attachment. The higher incubation time for initial colonization (~ 72 h), the delay in conditioning film proteins adsorption up to 48 h (Talluri et al. 2020) and the absence of conditioning film structures on PVC suggest that, among the PBR materials tested, this material should be explored as a potential antifouling material to delay and decrease the attachment of engineered *Anabaena*, and perhaps other bacteria.

In order to check the validity of the scratch and scan method in determining the thickness of the conditioning films, a sticky tape method was conducted on glass (Anderson 2009). Figure 7 shows the representative AFM topography image of the glass obtained by the sticky tape method after incubation in engineered *Anabaena* suspension for 96 h. The area under the sticky tape is shown on the left side and the conditioning film deposited on glass is shown on the right side of the image. The thickness of the conditioning films found from this method was 7.0 (± 1.8) nm on glass at 96 h which is close (Tukey's test, $p > .05$) to the thickness of 8.0 (± 0.2) nm obtained from the scratch and scan method. These results indicate that AFM can be used successfully, not only to determine the thickness of the conditioning films, but also to extract quantitative nanoscale information from the three-dimensional view of surfaces. This demonstrates important advantages of AFM over spectral ellipsometry which requires the input of physical properties such as the refractive index of the samples and the use of extensive mathematical models to determine the thickness of the films (Hong et al. 2011), making it difficult to analyze samples whose physical properties are unknown. Furthermore, accurate measurement of film thicknesses < 10 nm is difficult with spectral ellipsometry (Pascu and Dinescu 2012). The methods described in the present study can be applied to the examination of conditioning films formed by a diverse range of fouling organisms to better understand their adhesion mechanisms, leading to better control or prevention of biofouling, and to the development of antifouling materials.

It may be noted that the BG-11 medium used in this study is a commonly used growth medium for culturing cyanobacteria in commercial photobioreactors. On the other hand, no attempt was made to reproduce the varied and construction-dependent flow conditions of PBRs, which may certainly influence the development of conditioning films. All the PBR materials were incubated under static conditions without shaking or generating any flow conditions, so

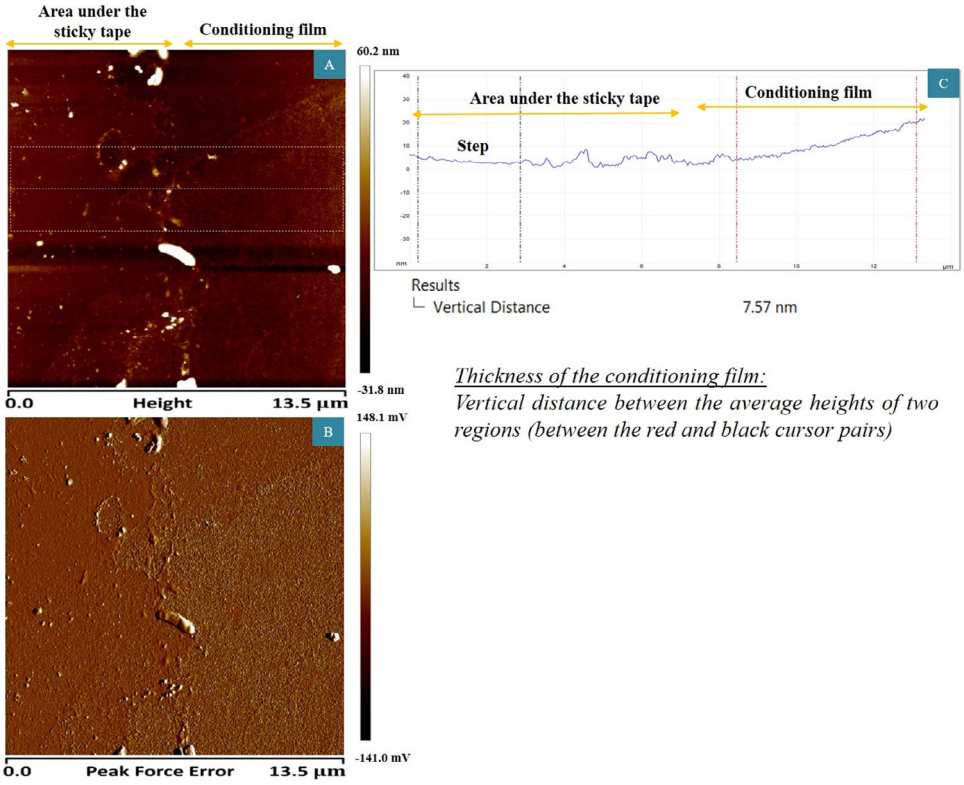

Figure 7. Representative AFM topography (A) and phase (B) images of glass obtained from the adhesive tape method. The right side of the image represents the conditioning film deposited on glass. The left side of the image shows the area that was under the sticky tape. The box indicated with the dashed lines in the topography image represents the region used for step analysis. (C) shows the result of the step analysis within this boxed region obtained in the form of average heights of the conditioning film and the area under the adhesive tape. The region between the black markers where the interference by the sticky residue of the tape appeared minimal was used as a step to determine the thickness of the conditioning films. The thicknesses of the conditioning film determined using step function in three different areas of each of the three replicate coupons were averaged. The average thickness of the conditioning film obtained by adhesive tape method was found to be 7.0 (± 1.8) nm on glass at 96 h. This value represents the mean ± the SE of the three-independent means (n = 3). Images were obtained with a scan area of 13.5 µm × 13.5 µm.

as to create a well-controlled baseline environment for the *Anabaena* cells to attach to the materials. This batch culture experiment was conducted with the goal of understanding the adhesion mechanisms of *Anabaena* and was not designed to mimic fluid movement in a PBR. Analysis of conditioning films formed under continuous flow of a growth medium, use of wastewater, and application of a CO_2 enriched environment may be foci of future investigations. The present work, and the related article (Talluri et al. 2020), will provide a valuable reference line for those studies.

Conclusions

Atomic force microscopy investigations of the physical appearance of conditioning films formed during engineered *Anabaena* cell adhesion revealed that the conditioning films were deposited as spikes/dot-like structures on most of the PBR materials. Time dependent changes in the surface roughness of the PBR materials did not have a significant effect on *Anabaena* cell attachment to the materials. The increase in thickness of the conditioning films with time was found to relate to the *Anabaena* attachment process on the PBR materials more accurately than surface roughness, and the formation time and extent of the adsorbed conditioning film spike structures were found to be material dependent. The higher surface area resulting from these spike-like structures may play a crucial role in providing effective adhesion sites for *Anabaena* attachment to PBR materials, resulting in efficient and quite rapid attachment of the bacterial cells on glass, PMMA, PC and HDPE. Conversely, the lack of conditioning film spikes and the insignificant change in thickness of the conditioning films with time on PVC may be related to the relative delay in both the adsorption of conditioning film proteins and the initial attachment of the engineered *Anabaena* cells on this surface. This result

suggests that further exploration of PVC for future consideration as an antifouling surface may be fruitful. The thickness of the conditioning films on glass measured by a scratch and scan method correlated well with the results obtained from the adhesive tape method, which indicates that both these methods could be used interchangeably, as advantageous alternatives to spectral ellipsometry. Altogether, the results from this AFM study demonstrate that analysis of the physical property changes during the adhesion of microorganisms on materials is as important as analyzing the surface chemistry changes by FTIR or XPS for gaining an improved understanding of the mechanisms involved in adhesion of bacteria to material surfaces and for further development of antifouling materials.

Disclosure statement

No potential conflict of interest was reported by the authors.

Funding

This work was financially supported by the National Aeronautics and Space Administration (NASA) under Grant number NNX11AM03A, the Department of Chemical and Biological Engineering (CBE) at the South Dakota School of Mines and Technology and the Composites and the Polymer Engineering (CAPE) Laboratory at South Dakota School of Mines and Technology and these organizations are gratefully acknowledged by the authors.

ORCID

David R. Salem http://orcid.org/0000-0003-4216-9405

References

Anderson EV. 2009. Polymer brush force modeling and experimentation. Worcester (MA): Worcester Polytechnic Institute. Project Number: PH-NAB-MP10.

Auerbach ID, Sorensen C, Hansma HG, Holden PA. 2000. Physical morphology and surface properties of unsaturated *Pseudomonas putida* biofilms. J Bacteriol. 182: 3809–3815. doi:10.1128/JB.182.13.3809-3815.2000

Beech IB, Smith JR, Steele AA, Penegar I, Campbell SA. 2002. The use of atomic force microscopy for studying interactions of bacterial biofilms with surfaces. Colloids Surf B Biointerfaces. 23:231–247. doi:10.1016/S0927-7765(01)00233-8

Beech IB, Sunner JA, Hiraoka K. 2005. Microbe-surface interactions in biofouling and biocorrosion processes. Int Microbiol. 8:157–168.

Bixler GD, Bhushan B. 2012. Biofouling: lessons from nature. Philos Trans A Math Phys Eng Sci. 370: 2381–2417. doi:10.1098/rsta.2011.0502

Brennan L, Owende P. 2010. Biofuels from microalgae—a review of technologies for production, processing, and extractions of biofuels and co-products. Renewable Sustainable Energ Rev. 14:557–577. doi:10.1016/j.rser.2009.10.009

Compere C, Bellon-Fontaine MN, Bertrand P, Costa D, Marcus P, Poleunis C, Pradier CM, Rondot B, Walls M. 2001. Kinetics of conditioning layer formation on stainless steel immersed in seawater. Biofouling. 17:129–145. doi:10.1080/08927010109378472

Costerton JW, Geesey GG, Cheng KJ. 1978. How bacteria stick. Sci Am. 238:86–95. doi:10.1038/scientificamerican0178-86

Cui Y, Yuan W, Cao J. 2013. Effects of surface texturing on microalgal cell attachment to solid carriers. Int J Agr Biol Eng. 6:44–54.

Dasgupta CN, Gilbert JJ, Lindblad P, Heidorn T, Borgvang SA, Skjanes K, Das D. 2010. Recent trends on the development of photobiological processes and photobioreactors for the improvement of hydrogen production. Int J Hydrogen Energy. 35:10218–10238. doi:10.1016/j.ijhydene.2010.06.029

De Philippis R, Sili C, Paperi R, Vincenzini M. 2001. Exopolysaccharide-producing cyanobacteria and their possible exploitation: a review. J Appl Phycol. 13: 293–299. doi:10.1023/A:1017590425924

De Philippis R, Vincenzini M. 1998. Exocellular polysaccharides from cyanobacteria and their possible applications. FEMS Microbiol Rev. 22:151–175. doi:10.1111/j.1574-6976.1998.tb00365.x

De Vree JH, Bosma R, Janssen M, Barbosa MJ, Wijffels RH. 2015. Comparison of four outdoor pilot-scale photobioreactors. Biotechnol Biofuels. 8:212–215. doi:10.1186/s13068-015-0400-2

Dragone G, Fernandes BD, Vicente AA, Teixeira JA. 2010. Third generation biofuels from microalgae. In: MéndezVilas A, editor. Current research, technology and education topics in applied microbiology and microbial biotechnology. Vol. 2. Spain: Formatex Research Center; p. 1355–1366.

Duke E. 2011. Cyanofactory platform to photosynthetically produce advanced fuels and chemicals, while providing bioregenerative life support services. (NASA Proposal Number. 11-EPSCoR-0051). Rapid City: South Dakota School of Mines and Technology.

Francius G, El Zein R, Mathieu L, Gosselin F, Maul A, Block J-C. 2017. Nano-exploration of organic conditioning film formed on polymeric surfaces exposed to drinking water. Water Res. 109:155–163. doi:10.1016/j.watres.2016.11.038

Gazze SA, Saccone L, Smits MM, Duran AL, Leake JR, Banwart SA, Ragnarsdottir KV, McMaster TJ. 2013. Nanoscale observations of extracellular polymeric substances deposition on phyllosilicates by an ectomycorrhizal fungus. Geomicrobiol J. 30:721–730. doi:10.1080/01490451.2013.766285

Genin SN, Aitchison JS, Allen DG. 2014. Design of algal film photobioreactors: material surface energy effects on algal film productivity, colonization and lipid content.

Bioresour Technol. 155:136–143. doi:10.1016/j.biortech.2013.12.060

Gesang T, Fanter D, Höper R, Possart W, Hennemann OD. 1995. Comparative film thickness determination by atomic force microscopy and ellipsometry for ultrathin polymer films. Surf Interface Anal. 23:797–808. doi:10.1002/sia.740231202

Harris L, Tozzi S, Wiley P, Young C, Richardson T-M, Clark K, Trent JD. 2013. Potential impact of biofouling on the photobioreactors of the Offshore Membrane Enclosures for Growing Algae (OMEGA) system. Bioresour Technol. 144:420–428. doi:10.1016/j.biortech.2013.06.125

Hong X, Gan Y, Wang Y. 2011. Facile measurement of polymer film thickness ranging from nanometer to micrometer scale using atomic force microscopy. Surf Interface Anal. 43:1299–1303. doi:10.1002/sia.3711

Hwang G, Kang S, El-Din MG, Liu Y. 2012a. Impact of an extracellular polymeric substance (EPS) precoating on the initial adhesion of *Burkholderia cepacia* and *Pseudomonas aeruginosa*. Biofouling. 28:525–538. doi:10.1080/08927014.2012.694138

Hwang G, Kang S, El-Din MG, Liu Y. 2012b. Impact of conditioning films on the initial adhesion of *Burkholderia cepacia*. Colloids Surf B Biointerfaces. 91:181–188. doi:10.1016/j.colsurfb.2011.10.059

Hwang G, Liang J, Kang S, Tong M, Liu Y. 2013. The role of conditioning film formation in *Pseudomonas aeruginosa* PAO1 adhesion to inert surfaces in aquatic environments. Biochem Eng J. 76:90–98. doi:10.1016/j.bej.2013.03.024

Irving TE, Allen DG. 2011. Species and material considerations in the formation and development of microalgal biofilms. Appl Microbiol Biotechnol. 92:283–294. doi:10.1007/s00253-011-3341-0

Ladner DA, Mei Seng EL C, Clark MM. 2010. Membrane fouling by marine algae in seawater desalination. Urbana (IL): University of Illinois at Urbana-Champaign. Evanston (IL): Northwestern University. Available from: Water Research Foundation, Arsenic Water Technology Partnership, WERC (USA).

Lobo RFM, Pereira-da-Silva MA, Raposo M, Faria RM, Oliveira ON, Pereira-da-Silva MA, Faria RM. 1999. In situ thickness measurements of ultra-thin multilayer polymer films by atomic force microscopy. Nanotechnology. 10:389–393. doi:10.1088/0957-4484/10/4/305

Lorite GS, de Souza AA, Neubauer D, Mizaikoff B, Kranz C, Cotta MA. 2013. On the role of extracellular polymeric substances during early stages of *Xylella fastidiosa* biofilm formation. Colloids Surf B Biointerfaces. 102:519–525. doi:10.1016/j.colsurfb.2012.08.027

Lorite GS, Rodrigues CM, De Souza AA, Kranz C, Mizaikoff B, Cotta MA. 2011. The role of conditioning film formation and surface chemical changes on *Xylella fastidiosa* adhesion and biofilm evolution. J Colloid Interface Sci. 359:289–295. doi:10.1016/j.jcis.2011.03.066

Mody BR, Bindra MO, Modi VV. 1990. Capsule development and structural characterization of acidic extracellular polysaccharides secreted by cowpea *Rhizobia*. Curr Microbiol. 20:145–152. doi:10.1007/BF02091989

Oliveira DR. 1992. Physico-chemical aspects of adhesion. In: Melo LF, Bott TR, Fletcher M, Capdeville B, editors. Biofilms—science and technology. Dordrecht (Netherlands): Springer; p. 45–58.

Ong CJ, Wong ML, Smit JOHN. 1990. Attachment of the adhesive holdfast organelle to the cellular stalk of *Caulobacter crescentus*. J Bacteriol. 172:1448–1456. doi:10.1128/jb.172.3.1448-1456.1990

Parmar A, Singh NK, Pandey A, Gnansounou E, Madamwar D. 2011. Cyanobacteria and microalgae: a positive prospect for biofuels. Bioresour Technol. 102:10163–10172. doi:10.1016/j.biortech.2011.08.030

Pascu R, Dinescu M. 2012. Spectroscopic ellipsometry. Rom Rep Phys. 64:135–142.

Preedy E, Perni S, Nipiĉ D, Bohinc K, Prokopovich P. 2014. Surface roughness mediated adhesion forces between borosilicate glass and gram-positive bacteria. Langmuir. 30:9466–9476. doi:10.1021/la501711t

Rasband WS. 1997–2018. ImageJ. Bethesda (MD): US National Institutes of Health. https://imagej.nih.gov/ij/.

Rippka R, Deruelles J, Waterbury JB, Herdman M, Stanier RY. 1979. Generic assignments, strain histories and properties of pure cultures of cyanobacteria. Microbiology. 111:1–61. doi:10.1099/00221287-111-1-1

Ruffing AM. 2011. Engineered cyanobacteria: teaching an old bug new tricks. Bioeng Bugs. 2:136–149. doi:10.4161/bbug.2.3.15285

Talluri SNL, Winter RM, Salem DR. 2020. Conditioning film formation and its influence on the initial adhesion and biofilm formation by a cyanobacterium on photobioreactor materials. Biofouling. 36:183–199. doi:10.1080/08927014.2020.1748186

Thomas DJ, Sullivan SL, Price AL, Zimmerman SM. 2005. Common freshwater cyanobacteria grow in 100% CO2. Astrobiology. 5:66–74. doi:10.1089/ast.2005.5.66

Thome I, Bauer S, Vater S, Zargiel K, Finlay JA, Arpa-Sancet MP, Alles M, Callow JA, Callow ME, Swain GW, et al. 2014. Conditioning of self-assembled monolayers at two static immersion test sites along the east coast of Florida and its effect on early fouling development. Biofouling. 30:1011–1021. doi:10.1080/08927014.2014.957195

Thome I, Pettitt ME, Callow ME, Callow JA, Grunze M, Rosenhahn A. 2012. Conditioning of surfaces by macromolecules and its implication for the settlement of zoospores of the green alga *Ulva linza*. Biofouling. 28:501–510. doi:10.1080/08927014.2012.689288

Uzum C, Hellwig J, Madaboosi N, Volodkin D, von Klitzing R. 2012. Growth behaviour and mechanical properties of PLL/HA multilayer films studied by AFM. Beilstein J Nanotechnol. 3:778–788. doi:10.3762/bjnano.3.87

van der Aa BC, Dufrene YF. 2002. In situ characterization of bacterial extracellular polymeric substances by AFM. Colloids Surf B Biointerfaces. 23:173–182. doi:10.1016/S0927-7765(01)00229-6

Wang B, Lan CQ, Horsman M. 2012. Closed photobioreactors for production of microalgal biomasses. Biotechnol Adv. 30:904–912. doi:10.1016/j.biotechadv.2012.01.019

Wang D, Wu X, Long L, Yuan X, Zhang Q, Xue S, Wen S, Yan C, Wang J, Cong W. 2017. Improved antifouling properties of photobioreactors by surface grafted sulfobetaine polymers. Biofouling. 33:970–979. doi:10.1080/08927014.2017.1394457

Yang Y, Wikieł AJ, Dall'Agnol LT, Eloy P, Genet MJ, Moura JJG, Sand W, Dupont-Gillain CC, Rouxhet PG. 2016. Proteins dominate in the surface layers formed on materials exposed to extracellular polymeric substances from bacterial cultures. Biofouling. 32:95–108. doi:10.1080/08927014.2015.1114609

Zeriouh O, Marco-Rocamora A, Reinoso-Moreno JV, López-Rosales L, García-Camacho F, Molina-Grima E. 2019. New insights into developing antibiofouling surfaces for industrial photobioreactors. Biotechnol Bioeng. 116:2212–2222. doi:10.1002/bit.27013

Zeriouh O, Reinoso-Moreno JV, López-Rosales L, Cerón-García MDC, Sánchez-Mirón A, García-Camacho F, Molina-Grima E. 2017. Biofouling in photobioreactors for marine microalgae. Crit Rev Biotechnol. 37:1006–1023. doi:10.1080/07388551.2017.1299681

Zhou R, Gibbons W. 2015. South Dakota State University, assignee. Mar 31. Genetically engineered cyanobacteria. United States patent US 8,993,303.